Geophysical Research Letters

RESEARCH LETTER
10.1029/2018GL077896

Key Points:
- The spatial distribution of ammonia oxidation was reported for the first time in the northern South China Sea
- Enhanced ammonia oxidation was associated with the Kuroshio Current intrusion
- Remineralization of DON introduced by the Kuroshio Current was likely a stimulator to enhance the ammonia oxidation in the northern South China Sea

Supporting Information:
- Supporting Information S1
- Table S1
- Data Set S1
- Figure S1
- Figure S2
- Figure S3
- Figure S4
- Figure S5
- Figure S6
- Figure S7

Correspondence to:
S.-J. Kao,
sjkao@xmu.edu.cn

Citation:
Xu, M. N., Zhang, W., Zhu, Y., Liu, L., Zheng, Z., Wan, X. S., et al. (2018). Enhanced ammonia oxidation caused by lateral Kuroshio intrusion in the boundary zone of the northern South China Sea. *Geophysical Research Letters*, *45*, 6585–6593. https://doi.org/10.1029/2018GL077896

Received 12 MAR 2018
Accepted 7 JUN 2018
Accepted article online 15 JUN 2018
Published online 5 JUL 2018

Enhanced Ammonia Oxidation Caused by Lateral Kuroshio Intrusion in the Boundary Zone of the Northern South China Sea

Min Nina Xu[1], Weijie Zhang[1], Yifan Zhu[1], Li Liu[1], Zhenzhen Zheng[1], Xianhui Sean Wan[1], Wei Qian[1], Minhan Dai[1], Jianping Gan[2], David A. Hutchins[3], and Shuh-Ji Kao[1]

[1]State Key Laboratory of Marine Environmental Science, College of Ocean and Earth Sciences, Xiamen University, Xiamen, China, [2]Department of Mathematics and Division of Environment, Hong Kong University of Science and Technology, Kowloon, Hong Kong, [3]Marine and Environmental Biology, Department of Biological Sciences, University of Southern California, Los Angeles, CA, USA

Abstract Lateral input of dissolved organics may play a significant role to support productivity in oligotrophic ocean although associated biogeochemical evidences are lacking in the field. Ammonia oxidation (AO), the first step of nitrification that bridges organic remineralization and nitrate, is potentially an immediate responder. By using $^{15}N\text{-}NH_4^+$, the spatial distribution of AO was investigated in the northern South China Sea, where Kuroshio Current intrudes frequently. AO ranged widely (0.001 to 134 nmol $\cdot L^{-1} \cdot day^{-1}$) in space and the depth-integrated (200 m) AO peaked where the Kuroshio influence is moderate suggesting that enhanced AO had occurred due to lateral mixing. Since oligotrophic Kuroshio is characterized by high dissolved organic nitrogen (DON), such lateral mixing not only introduces external DON into the northern South China Sea but also enhances NH_4^+ regeneration and subsequent oxidation to complicate the conventional new production in the boundary zone with DON gradient.

Plain Language Summary The horizontal mixing is widespread in oligotrophic ocean; however, the mixing-induced biogeochemical response is hard to detect and remains less explored. We measured ammonia oxidation (AO), a critical process immediately responds to remineralization of dissolved organic matter (DOM), along the pathway of Kuroshio intrusion into the South China Sea. We found AO peaked at stations where the influence of Kuroshio Current intrusion is moderate. We hypothesized that intrusion of oligotrophic water brings on-site recalcitrant DOM into marginal seas and enriches ammonium level via bacteria decomposition of the foreign DOM. Accompanied is the enhancement of AO, which transfers DOM into nitrate, further complicating the conventional concept of N-based new production. Such lateral intrusion or transport appears also along a meridional direction. For example, the western boundary current (warm and saline) carrying DOM-rich water flows toward higher latitudes where nutrients are high. According to our findings, such hemispheric scale transport may exert considerable influence on high-latitude nitrogen biogeochemistry. Knowledge of the impact of Kuroshio intrusion on AO in the northern South China Sea was a step forward in documenting this type of response in frontal zone, but more studies will be needed to validate the underlying mechanisms.

1. Introduction

Nitrogen (N) plays a prominent role in oceanic biogeochemistry, as it is tightly coupled with various elemental cycles, particularly carbon and phosphorus (Gruber, 2008). Among various N forms, nitrate (NO_3^-) dominates the bioavailable nitrogen reservoir in the deep ocean, and the vertical supply of NO_3^- largely controls marine productivity in the euphotic ocean (Falkowski, 1997; Moore et al., 2013; Tyrrell, 1999). This vertical NO_3^- transport contributes to new production as defined by Dugdale and Goering (1967) in regions less influenced by atmospheric deposition and N_2 fixation. On the other hand, ammonium (NH_4^+) is recycled rapidly in oligotrophic surface ocean, acting as the primary recycled N source to sustain regenerated production (Dugdale & Goering, 1967; Eppley et al., 1973).

Besides vertical NO_3^- supply from deep ocean, lateral input of dissolved organic matter (DOM, dissolved organic carbon or nitrogen, DOC/DON) must be considered as an important process for nutritional supplement. It transports additional *new nutrients* to oligotrophic regions, such as the center of the subtropical gyre (Abell et al., 2000; Bacastow & Maier-Reimer, 1991; Mahaffey et al., 2004; Peltzer &

Hayward, 1996). Some model results show that horizontal advection of such new nutrients is comparable or exceeded the vertical transport of inorganic nutrients in at least some regions (Anderson et al., 2015, and references therein; Letscher et al., 2016). In spite of the potential importance of such lateral advection of DOM, field investigations of associated biogeochemical responses, particularly nitrogen cycle processes, are still lacking.

Nitrification is one of the most important N transformation processes in the N cycle, as it links the most reduced form (NH_4^+) with the most oxidized form (NO_3^-) and can produce the strong greenhouse gas nitrous oxide as a byproduct (Ward, 2008, 2011). In the sunlit ocean, remineralization-produced NH_4^+ may be transformed to NO_3^- via nitrification and the newly produced recycled NO_3^- may refuel the phytoplankton uptake. If this pathway proceeds in euphotic ocean, it may not only regulate the distribution of N species and thus the community structure responsible for productivity but also influence the estimation of conventionally defined new production (Yool et al., 2007).

The South China Sea (SCS) is the largest marginal sea in the world, and its surface circulation pattern varies seasonally according to monsoons (e.g., Li, 2008; Shaw & Chao, 1994; Wong et al., 2007). A branch of the western boundary current, Kuroshio Current (KC), intrudes into the northern SCS (NSCS) seasonally when passing by the Luzon Strait (Nan et al., 2015, and references therein) (Figure 1a). Encountering the warm, nutrient-depleted, and DOM-rich KC, the NSCS provides a good experimental ground to explore the response of ammonia oxidation (AO) to the lateral intrusion of oligotrophic water. The Kuroshio intrusion (KI) occurs year round, though it varies in magnitude and has been shown to influence the nutrient biogeochemistry of the upper 100 m in the NSCS through dilution of inorganic nutrients (Du et al., 2013) and enrichment of DOC (Wu et al., 2015). Using ^{15}N-labeled NH_4^+ addition techniques, this study provides the first information on the spatial distribution of AO and the potential mechanism for lateral advection of water mass to modulate AO in the boundary zone of the NSCS.

2. Material and Methods

2.1. Sample Collection and Measurements

The cruise was conducted during 15 May through 7 June 2016 on the R/V *Dongfanghong II* in the NSCS. Samples were collected by using a 24-bottle Niskin rosette system with 12-L PVC bottles, equipped with a SeaBird conductivity-temperature-depth. Samples for NH_4^+, NO_2^-, and NO_3^- concentration were preserved in 50-mL polypropylene centrifuge tubes (BD FALCON) at −20 °C without filtration until analysis. In total, 48 stations covering the shelf and the route of the KI were probed by conductivity-temperature-depth to assess the chemical hydrography influenced by the Kuroshio in spatial scale. Among the 48 stations, 13 were selected for AO measurement to explore the Kuroshio impact on the spatial distribution of AO (Figures 1 and S1 in the supporting information).

NH_4^+ concentrations were analyzed by using the fluorometric *o*-phthaldialdehyde method with a detection limit of 0.7 nmol/L (Zhu et al., 2013). Samples for NO_2^- and NO_3^- concentrations (μM level) were determined by classical colorimetric methods with a Technicon Auto-Analyzer III (AA3, Bran-Luebbe). The detection limits for NO_2^- and NO_3^- were 0.02 and 0.07 μmol/L, respectively (Dai et al., 2008). For low-level NO_2^- and NO_3^-, we used flow injection analysis-liquid waveguide capillary cell method with a detection limit of 2 nmol/L (Patey et al., 2008).

2.2. Estimate of Kuroshio Fraction

To quantify the hydrographic change induced by lateral KI, we applied an isopycnal mixing model (Du et al., 2013) to calculate the fractional contribution of Kuroshio water in every individual water sample. The model is under the assumption that diapycnal mixing is negligible when compared with isopycnal mixing (see supporting information). In the isopycnal model, two end-members are required for index estimation. Here we selected the SEATS station at 116°E/18°N to represent the proper SCS water mass end-member and P4 station at 122.959°E/20.003°N for the Kuroshio water mass end-member (see Figure 1a for locations and discussions of end-member selection). According to the assumption, we can quantify the proportion of the SCS (R_S) and the Kuroshio (R_K) water for any observed water parcel in the θ–S diagram in Figure S1, basing on the conservation of either potential temperature (θ) or salinity (S) along an isopycnal surface (See profiles in Figure S2.):

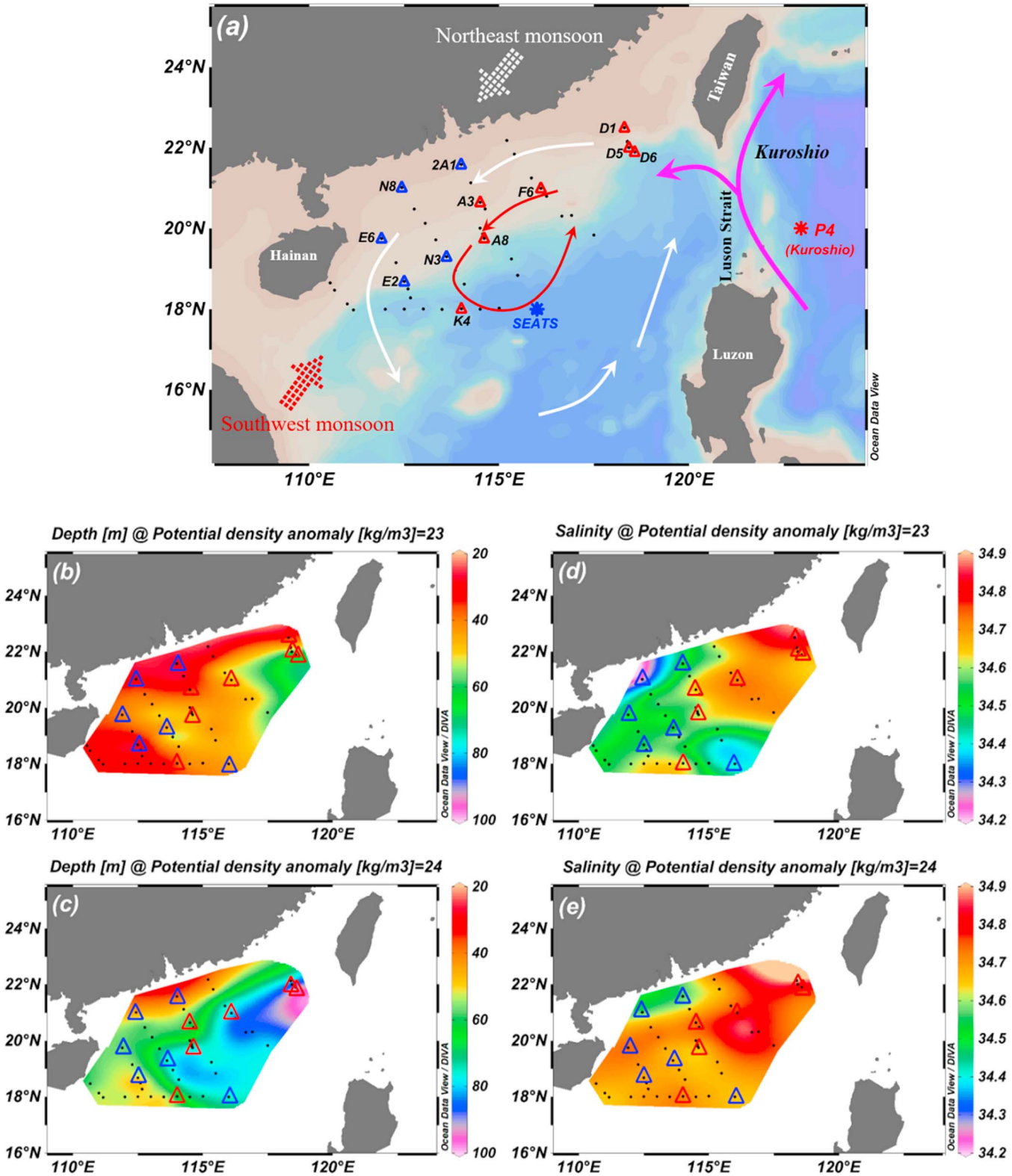

Figure 1. Study area and sampling stations during the 2016 summer cruise in the northern South China Sea. The white and red arrows stand, respectively, for the wintertime and summertime surface circulation in northern South China Sea. The solid dots are for CTD sampling stations. The red and blue triangles in panel (a) are for ammonia oxidation incubation stations featured with more and less Kuroshio water influence, respectively (see text; and the same in the following figures). The SEATS and P4 are the two end-members used in the mixing model; and (b–e) showing the spatial distributions of depth and salinity of isopycnal surface of the potential density anomaly (σ_θ) of 23 and 24 kg/m^3. CTD = conductivity-temperature-depth.

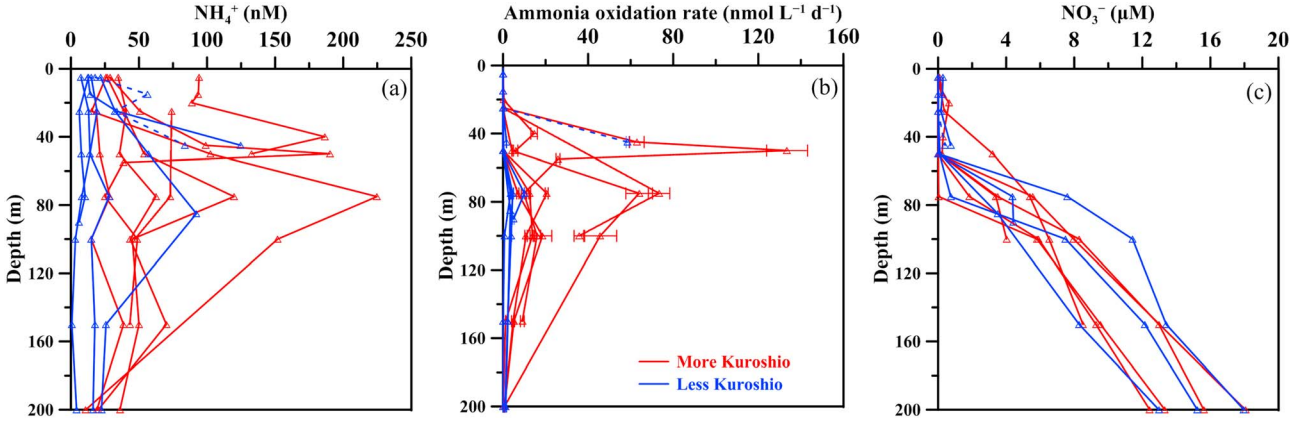

Figure 2. The vertical profiles of (a) NH_4^+ concentration (nmol N/L), (b) ammonia oxidation rate (nmol $N \cdot L^{-1} \cdot day^{-1}$), and (c) nitrate at ammonia oxidation incubation stations. The dashed blue line is data for N8 station.

$$R_K + R_S = 1, \tag{1}$$

$$R_K \times \theta_K + R_S \times \theta_S = \theta \text{ or } R_K \times S_K + R_S \times S_S = S. \tag{2}$$

Note that the fractional contribution from end-member varies according to end-member selections. Though we named P4 "Kuroshio," the R_K values were just used to describe the relative contributions from P4, rather than providing absolute contribution from "typical Kuroshio" water mass (see more details of isopycnal model in Text S1). On the other hand, the vertical mixing during lateral transport may violate the assumption of isopycnal mixing (see Text S1). In the NSCS, however, the mixed layer depth occupied a limited fraction while we integrate/average R_K values throughout the upper 100-/200-m water column. Thus, the influence of mixed layer depth on R_K estimation is negligible at least in our study.

2.3. Incubation Experiments

Duplicate water samples for AO rate measurements were collected from four to eight depths in the upper 200 m (shown in Figure 2). For more accurate rate measure, we followed the protocol in Ward et al. (1989). For each sample, 250 mL HDPE bottle was injected with $^{15}NH_4Cl$ plus carrier $Na^{14}NO_2$ to reach final concentrations of 50 nmol/L for $^{15}NH_4Cl$ and 1 μmol/L for $Na^{14}NO_2$. After tracer addition and homogeneous mixing, ~45 mL water was immediately taken out from the incubation bottle and then filtered through a 0.22 μm disposable syringe filter. The filtrates were frozen to serve as t_0 samples. The remaining water in the incubation bottle was dark, incubated in a thermostat incubator at in situ temperature. Incubations were ended by filtration (0.22 μm filter) after 12 hr, except samples from one station (K4), which were incubated for 12, 24, and 36 hr.

2.4. Isotope Measurement and Rate Calculation

The isotopic composition of NO_2^- was measured at t_0 and at the end of the incubations. Rates of AO were thus calculated according to the net accumulation of ^{15}N in NO_2^- during the incubations. The effect of biological fractionation is assumed to be negligible during incubation. To determine $\delta^{15}N\text{-}NO_2^-$, we followed the protocol of McIlvin and Altabet (2005). NO_2^- was first quantitatively converted into N_2O by a helium-purged 1:1 (v:v) solution of 2 mol/L NaN_3 and 20% acetic acid. The isotopic composition of the N_2O produced was measured by a gasbench coupled with an isotope ratio mass spectrometer (Thermo Delta V Advantage).

Rates were calculated according to equation (3):

$$R = \frac{r_t \times [NO2-]_t - r_0 \times [NO2-]_0}{T} \times \frac{1}{F}, \tag{3}$$

where R is the AO rate (nmol $\cdot L^{-1} \cdot day^{-1}$), r_t and r_0 are the ^{15}N fractions in NO_2^- (defined as $^{15}N/(^{15}N + {}^{14}N)$) at the end and the start of the incubation, respectively; $[NO_2^-]_t$ and $[NO_2^-]_0$ stand for NO_2^- concentrations (nmol/L) at the end and the start, respectively; T is the period of incubation (hr) and F is the fraction of NH_4^+ labeled with ^{15}N at the start of incubation.

To ensure the accuracy and reliability of rate measure, we conducted time course incubations. The rate of ^{15}N accumulation in the end-product ($^{15}N\text{-}NO_2^-$) over time course incubation was then used for in situ AO rate derivation. For example, at Station K4 (Figure S3), $^{15}N\text{-}NO_2^-$ increased with elapsed time, displaying significant linear pattern for all depths although the rate value (slope) varied from as low as 0.0002 up to 0.58 nmol $\cdot L^{-1} \cdot hr^{-1}$. Such strong linear regression patterns affirmed the data reliability.

3. Results and Discussions

As the KC is characterized by warm and saline surface water, the zonal distribution of salinity in a contour plot can be used to reveal the spatial pattern of KI. The contours of the depth of the isopycnal layer (potential density anomaly (σ_θ) of 23 and 24 in Figures 1b and 1c, respectively) showed a shoaling pattern toward the west, agreeing with previous findings that the SCS is a basin-scale upwelling system (Wong et al., 2007). A clear intrusion pattern of high-salinity water to the east near the Luzon Strait can be seen in salinity contours (Figures 1d and 1e) specifically at given σ_θ of 23 and 24. Similar intrusion patterns have been reported previously (Du et al., 2013). Accordingly, the upwelled subsurface SCS water may introduce nutrients and bacteria into Kuroshio water during the lateral intrusion into the NSCS.

Except for very near surface water at a few stations (influenced by rainfall or riverine freshwater), θ and S of all the sampling stations fell well within the field between the two end-members (red and blue curves in Figure S1a), indicating that we may properly evaluate the Kuroshio influence using this two-end-member model. Station N8, which contained a significant freshwater signal located on the shallow shelf (Figure 1a), was viewed as lacking Kuroshio influence (i.e., R_K of zero) and thus not taken into account in the two-end-member model (yellow dots in Figure S1a). In Figure S1b, the degree of Kuroshio influence can be seen clearly from the color, which represents the value of R_K, distribution in the θ-S diagram.

The degree of KI influence varied vertically. The vertical distributions of the R_K for the AO sampling stations are depicted in Figure S4. For the mixed layer with uniform θ or S, we can see uniform R_K in the surface about 10–40 m. Generally, R_K showed relative higher values in the upper 100 m with subsurface lows near 100 m (horizontal dashed line in Figure S4) and then increased with depth (Figure S4). Since the most intensive biological activities like photosynthetic production, regeneration, and export production processes occur in the euphotic ocean (e.g., Fawcett et al., 2015; Karl et al., 2001; Lipschultz, 2001; Tseng et al., 2005), which is usually defined by 1% of photosynthetically active radiation (PAR; Kirk, 1994). Moreover, in most of oligotrophic ocean in low latitude, the annual mean depth of 1% sPAR is ~100 m (94.3 ± 12.3 m at BATS based on Siegel et al., 1995; 75–94 m at SEATS station based on Tseng et al., 2005); thus, the selection of 100 m for integration is reasonable. Moreover, the average R_K for upper 200 m resembles that of the 100 m (Figure S6a). Thus, the depth average R_K of upper 100 m ($R_{K\text{ave-}100}$) can be a proper indicator to assess the influence of KC intrusion on sampling stations in the NSCS although the KC intrusion may deepen to 400 m (e.g., Tian et al., 2006).

The spatial contour of $R_{K\text{ave-}100}$ showed a distinct zonal distribution with higher values to the east (Figure S5), resembling the spatial distribution pattern of salinity. In the study region, the maximum $R_{K\text{ave-}100}$ was ~0.8. As mentioned above, R_K may vary as changing the two end-members. Therefore, the criterion of 0.35 was just set as a boundary for more and less Kuroshio influence for convenient discussion and to portray data point distribution in figures (see discussions in Text S1). Accordingly, Stations D1, D6, D5, F6, A3, K4, and A8 ($R_{K\text{ave-}100} > 0.35$) were classified as more Kuroshio-influenced stations (Figure S5 and Table S1).

Vertical NH_4^+ concentrations ranged from 0.7 to 224 nmol/L, with two distinct distribution patterns. One showed a subsurface maximum, while the other displayed no significant vertical structure (Figure 2a). In general, both NH_4^+ concentration (average of vertical profile) and inventory (depth integration for upper 200 m) for more Kuroshio-influenced stations (59 ± 49 nmol/L for concentration; 9,034 ± 4,803 μmol/m^2 for depth integration) were significantly higher than those of less Kuroshio-influenced stations (23 ± 27 nmol/L and 2,995 ± 2,861 μmol/m^2, respectively; Figure 2a and Table S1; for one-way ANOVA, $P = 0.021 < 0.05$). In addition to reported μM level inorganic nutrient dilution and DOC additions (Du et al., 2013; Wu et al., 2015), our results further suggested that KC intrusion is accompanied by higher NH_4^+ concentrations, although at nM levels. Whether the NH_4^+ was directly brought by KC or induced by postintrusion warrants further examination.

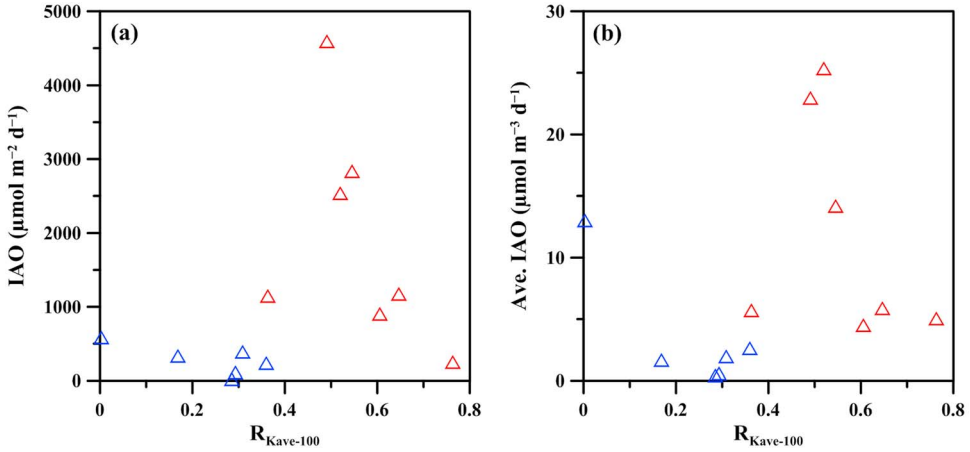

Figure 3. The scatter plot of (a) depth-integrated (upper 200 m) ammonia oxidation rate (IAO, μmol N · m^{-2} · day^{-1}) and (b) average ammonia oxidation rate (μmol N · m^{-3} · day^{-1}) against average Kuroshio fraction in upper 100 m.

As NH_4^+ is the initial substrate for AO, the KC intrusion-associated NH_4^+ enhancement probably stimulates the AO rate, with implications for the proportion of new and regenerated production in the NSCS. In Figure 2b, we present vertical profiles of in situ AO rate. AO was slow in surface layers (0.001–0.6 nmol · L^{-1} · day^{-1}) with high values ranging from 3.5 to 133.5 nmol · L^{-1} · d^{-1} at depths of ~40 to 100 m. Such downward increasing trend had been observed in previous studies and been attributed to light inhibition (Ward, 2005) and ambient nitrate concentration (Wan et al., 2018). Here in this study, AO appeared at around nitracline being consistent to previous observations. Below the depth of the AO rate maximum, rates decreased gradually with depths (Figure 2b). The AO rate at the N8 station influenced by freshwater (blue dashed line) was low at the surface and high at the bottom depths. Similar to the distribution pattern of NH_4^+, higher AO rates appeared at stations with higher Kuroshio influence (Figure 2b). In contrast to NH_4^+ concentration and AO, there is no significant difference in [NO_3^-] profile for more and less KC-influenced stations (Figure 2c), suggesting that in horizontal scale nitrate is not a major driver for AO enhancement. Although the nitrate profiles showed no distinctive difference, the nitrate inventory of upper 100 m roughly revealed an inverse correlation with $R_{kave\text{-}100}$ (Figure S6a), being consistent with the dilution effect indicated by Du et al. (2013).

According to results and discussions above, we further integrated AO rates for the water column (IAO) and estimated the depth-averaged AO (Ave. IAO) to explore the KI influence on NH_4^+ inventory and AO rate in the upper water column. Statistical results for the upper 200 m showed rates at more Kuroshio-influenced stations (251–4,594 μmol · m^{-2} · day^{-1} for IAO; 4.5–25.3 μmol · m^{-3} · day^{-1} for Ave. IAO) were significantly larger than those at less influenced stations (18.1–333.6 μmol · m^{-2} · day^{-1} and 0.4–2.6 μmol · m^{-3} · day^{-1}, respectively; for one-way ANOVA, $P = 0.022 < 0.05$). The upper 100 m integrated and averaged AO rates followed the same trend as those for the upper 200 m, being consistent with the R_K influence for both 100 and 200 m (Table S1).

As aforementioned, oligotrophic KI may dilute the NO_3^- inventory in the upper 100 m, thus, may diminish new production in NSCS and promote the ecological role of recycling nitrogen, that is, NH_4^+, in sustaining the system. To identify the source of this NH_4^+ is critical to understanding the function of this western boundary current intrusion. We plotted these integrated rate values (IAO and Ave. IAO) for the upper 200 m against $R_{Kave\text{-}100}$ to examine and evaluate the KI impact on the AO distribution. Results showed an inverse V shape, and surprisingly the AO peaked at moderate $R_{Kave\text{-}100}$ (0.35–0.70; see Figure 3) rather than at the highest $R_{Kave\text{-}100}$ end. Thus, the elevated AO signal was not directly carried by the Kuroshio. The only exception not following the inverse V pattern was the coastal station N8 on the *Y* axis (the symbols at $R_{Kave\text{-}100} = 0$ in Figure 3) that was influenced by freshwater. Additionally, the average R_K for the upper 200 m ($R_{Kave\text{-}200}$) showed a good positive correlation with that in the upper 100 m, with a slope of 1.01 ± 0.09 ($P < 0.0001$; Figure S6b). The upper 200 m integrated and averaged IAO rates (IAO and Ave. IAO)

plotted against $R_{Kave\text{-}200}$ (Figures S6c and S6d) showed the same pattern with rates as against average R_K of the upper 100 m in Figure 3. Such consistency further illustrated that the conclusion of postintrusion induced AO enhancement would not be biased by the depth range selected for integration.

The Kuroshio water, featured with higher potential temperature and salinity, is well known to hold low inorganic nutrients (Du et al., 2013). By contrast, DOC in the upper 200 m was significantly higher than that of the NSCS (51–70 μmol/L in NSCS and 60–79 μmol/L of Kuroshio water). The annual averaged TOC inventory in the central NSCS (~6.7 mol/m^2) was significantly lower than that in the Kuroshio (7.5 mol/m^2), indicating that the KC intrusion would increase the TOC inventory in the upper 100 m of the NSCS (Wu et al., 2015). Similarly, higher DON was also observed at more Kuroshio water influenced stations (5.4 ± 0.6 μmol/L) than at more SCS water-influenced stations (2.9 ± 1.2 μmol/L on average; Figure S7 and Table S3). Thus, we hypothesized that the high DOM brought by the Kuroshio water is recalcitrant to the Kuroshio-carried bacteria; however, Kuroshio DOM is bioavailable to bacteria dwelling in the SCS. A similar hypothesis had been proposed previously by Carlson et al. (2011) and Letscher et al. (2013), who found that refractory DOM at one place may be bioavailable for microbes at another site. Whether the DOM sourced from KC is bioavailable to bacteria living in NSCS required further tests; nevertheless, high-throughput rRNA sequence analyses of biological samples from NSCS and the Luzon Strait showed diverse community in the upper 100 m (Zhang et al., 2014). On the other hand, Shiah et al. (1998) showed that DOC degradation in western equatorial Pacific was stimulated by inorganic nutrient addition. Consequently, the relatively high-surface DOC in the western equatorial Pacific relative to the central equatorial Pacific was due to a shortage of inorganic nutrient supply, thus resulting in sluggish DOC degradation. Such phenomenon of inorganic nutrient limitation of DOM degradation was confirmed by subsequent studies (Berthelot et al., 2015; Van Wambeke et al., 2016), suggesting that nutrient limitation is an important factor for DOM accumulation.

From the depth distribution on the isopycnal surface of 23 and 24 (Figures 1b and 1c), the intruded Kuroshio water shoaled westward and mixed with the uplifted SCS water. Physical mixing-induced nutrient supply and nonlocal bacteria inoculation might activate remineralization and ammonification of DON in a manner similar to the studies cited above, thus, produced NH_4^+ for microbial use. Enhanced AO in waters within intermediate $R_{Kave\text{-}100}$ (0.35–0.70) supports this notion. More specifically, DON was insufficient in water with $R_{Kave\text{-}100} < 0.35$, while DON was high yet refractory for the on-site bacteria in water with $R_{Kave\text{-}100} > 0.7$.

The newly produced NH_4^+ may be consumed either by nitrifiers or by phytoplankton. If the NH_4^+ was directly oxidized by ammonia oxidizers, the NO_3^- produced by enhanced AO in the euphotic zone is involved directly in *new production*. Alternatively, if nitrifiers were outcompeted by phytoplankton in the sunlit ocean (Smith et al., 2014), the remineralized NH_4^+ was taken up by phytoplankton. Whether this production induced by lateral input of new DON can be exported out of the euphotic zone remains uncertain; however, the regeneration of NH_4^+ underneath may also stimulate AO. The enhanced NH_4^+ regeneration and subsequent AO rates, which is caused by lateral intrusion of the oligotrophic KC, is absolutely a significant yet hitherto unexplored process in the boundary zone regardless of the mechanism behind.

As high N_2 fixation rates and high *Trichodesmium* abundance in the route of KC were reported (Chen et al., 2008, 2013; Shiozaki et al., 2014), we may argue diazotrophs' release could be a direct source of NH_4^+ (Capone et al., 1994; Mulholland et al., 2004) to stimulate AO. If so, AO rates would be positively correlated with R_K, that is, the maximum AO rates appeared at the highest R_K but not at R_K with medium values. This is apparently not the case since nitrification did not peak in waters with the highest R_K value.

4. Conclusion

This is the first report of AO distribution in the NSCS. We found distinct spatial distributions of NH_4^+ concentrations and oxidation rates associated with the KI. Lateral transport of oligotrophic water brings on-site recalcitrant organic nitrogen into marginal seas and enriches NH_4^+ level via bacteria decomposition of the foreign DON. Enhancement of NH_4^+ production and oxidation further complicate the conventional concept of N-based new and regenerated production. Such lateral intrusion or transport may appear elsewhere with DON and nutrient gradients. Knowledge of the impact of KI on AO in the NSCS was a step forward in documenting this type of response, but more studies will be needed to validate the real underlying mechanisms.

Acknowledgments

This research was funded by the National Natural Science Foundation of China (NSFC 91328207, U1305233, 2015CB954003, and NSFC41503069). We sincerely thank all crew members of R/V *Dongfanghong II*, Wenbin Zou and Li Tian in Xiamen University for their assistance. We thank T.Y. Lee at National Taiwan Normal University for his help in calculating R_K using two end-member model. The MEL contribution number is melpublication 2017244. The data in this study were listed in the supporting information (Tables S1–S3). The authors declare no conflict of interest.

References

Abell, J., Emerson, S., & Renaud, P. (2000). Distributions of top, ton and toc in the North Pacific subtropical gyre: Implications for nutrient supply in the surface ocean and remineralization in the upper thermocline. *Journal of Marine Research*, *58*(2), 203–222. https://doi.org/10.1357/002224000321511142

Anderson, T. R., Christian, J. R., & Flynn, K. J. (2015). Modeling DOM biogeochemistry. In D. A. Hansell, & C. A. Carlson (Eds.), *Biogeochemistry of Marine Dissolved Organic Matter* (Vol. 15, pp. 635–667). UK and USA: Academic Press. https://doi.org/10.1016/B978-0-12-405940-5.00015-7

Bacastow, R., & Maier-Reimer, E. (1991). Dissolved organic carbon in modeling oceanic new production. *Global Biogeochemical Cycles*, *5*(1), 71–85. https://doi.org/10.1029/91GB00015

Berthelot, H., Moutin, T., L'Helguen, S., Leblanc, K., Hélias, S., Grosso, O., et al. (2015). Dinitrogen fixation and dissolved organic nitrogen fueled primary production and particulate export during the VAHINE mesocosm experiment (New Caledonia lagoon). *Biogeosciences*, *12*(13), 4099–4112. https://doi.org/10.5194/bg-12-4099-2015

Capone, D. G., Ferrier, M. D., & Carpenter, E. J. (1994). Amino acid cycling in colonies of the planktonic marine cyanobacterium *Trichodesmium thiebautii*. *Applied and Environmental Microbiology*, *60*(11), 3989–3995.

Carlson, C. A., Hansell, D. A., & Tamburini, C. (2011). DOC persistence and its fate after export within the ocean interior. In N. Z. Jiao, F. Azam, & S. Sanders (Eds.), *Microbial Carbon Pump in the Ocean* (Vol. 2011, pp. 57–59). Washington, DC: The American Association for the Advancement of Science. https://doi.org/10.1126/science.opms.sb000

Chen, Y. L. L., Chen, H. Y., Lin, Y. H., Yong, T. C., Taniuchi, Y., & Tuo, S. H. (2013). The relative contributions of unicellular and filamentous diazotrophs to N_2 fixation in the South China Sea and the upstream Kuroshio. *Marine Chemistry*, *85*, 56–71. https://doi.org/10.1016/j.dsr.2013.11.006

Chen, Y. L. L., Chen, H. Y., Tuo, S. H., & Ohki, K. (2008). Seasonal dynamics of new production from *Trichodesmium* N_2 fixation and nitrate uptake in the upstream Kuroshio and South China Sea basin. *Limnology and Oceanography*, *53*(5), 1705–1721. https://doi.org/10.4319/lo.2008.53.5.1705

Dai, M., Wang, L., Guo, X., Zhai, W., Li, Q., He, B., & Kao, S. J. (2008). Nitrification and inorganic nitrogen distribution in a large perturbed river/estuarine system: The Pearl River estuary, China. *Biogeosciences*, *5*(5), 1227–1244. https://doi.org/10.5194/bg-5-1227-2008

Du, C., Liu, Z., Dai, M., Kao, S.-J., Cao, Z., Zhang, Y., et al. (2013). Impact of the Kuroshio intrusion on the nutrient inventory in the upper northern South China Sea: Insights from an isopycnal mixing model. *Biogeosciences*, *10*(10), 6419–6432. https://doi.org/10.5194/bg-10-6419-2013

Dugdale, R., & Goering, J. (1967). Uptake of new and regenerated forms of nitrogen in primary productivity. *Limnology and Oceanography*, *12*(2), 196–206. https://doi.org/10.4319/lo.1967.12.2.0196

Eppley, R. W., Renger, E. H., Venrick, E. L., & Mullin, M. M. (1973). A study of plankton dynamics and nutrient cycling in the central gyre of the north Pacific Ocean. *Limnology and Oceanography*, *18*(4), 534–551. https://doi.org/10.4319/lo.1973.18.4.0534

Falkowski, P. G. (1997). Evolution of the nitrogen cycle and its influence on the biological sequestration of CO_2 in the ocean. *Nature*, *387*(6630), 272–275. https://doi.org/10.1038/387272a0

Fawcett, S. E., Ward, B. B., Lomas, M. W., & Sigman, D. M. (2015). Vertical decoupling of nitrate assimilation and nitrification in the Sargasso Sea. *Deep Sea Research Part I*, *103*, 64–72. https://doi.org/10.1016/j.dsr.2015.05.004

Gruber, N. (2008). The marine nitrogen cycle: Overview and challenges. In D. A. Capone, D. A. Bronk, M. R. Mulholland, & E. J. Carpenter (Eds.), *Nitrogen in the marine environment* (Vol. 1, pp. 1–50). London, UK: Academic Press.

Karl, D. M., Bidigare, R. R., & Letelier, R. M. (2001). Long-term changes in plankton community structure and productivity in the North Pacific subtropical gyre: The domain shift hypothesis. *Deep Sea Research Part II: Topical Studies in Oceanography*, *48*(8–9), 1449–1470.

Kirk, J. T. O. (1994). *Light and photosynthesis in aquatic ecosystems*. New York: Cambridge University Press.

Letscher, R. T., Hansell, D. A., Carlson, C. A., Lumpkin, R., & Knapp, A. N. (2013). Dissolved organic nitrogen in the global surface ocean: Distribution and fate. *Global Biogeochemical Cycles*, *27*, 141–153. https://doi.org/10.1029/2012GB004449

Letscher, R. T., Primeau, F., & Moore, J. K. (2016). Nutrient budgets in the subtropical ocean gyres dominated by lateral transport. *Nature Geoscience*, *9*(11), 815–819. https://doi.org/10.1038/ngeo2812

Li, L. (2008). Upper layer circulation in the South China Sea. In A. K. Liu, C.-R. Ho, & C.-T. Liu (Eds.), *Satellite remote sensing of South China Sea* (Chap. 18, pp. 275–290). Taipei: Tingmao Pub. Co. http://140.112.114.62/handle/246246/230294

Lipschultz, F. (2001). A time-series assessment of the nitrogen cycle at bats. *Deep Sea Research Part II: Topical Studies in Oceanography*, *48*(8–9), 1897–1924. https://doi.org/10.1016/S0967-0645(00)00168-5

Mahaffey, C., Williams, R. G., Wolff, G. A., & Anderson, W. T. (2004). Physical supply of nitrogen to phytoplankton in the Atlantic Ocean. *Global Biogeochemical Cycles*, *18*, GB1034. https://doi.org/10.1029/2003GB002129

McIlvin, M. R., & Altabet, M. A. (2005). Chemical conversion of nitrate and nitrite to nitrous oxide for nitrogen and oxygen isotopic analysis in freshwater and seawater. *Analytical Chemistry*, *77*(17), 5589–5595. https://doi.org/10.1021/ac050528s

Moore, C. M., Mills, M. M., Arrigo, K. R., Bermanfrank, I., Bopp, L., Boyd, P. W., et al. (2013). Processes and patterns of oceanic nutrient limitation. *Nature Geoscience*, *6*(9), 701–710. https://doi.org/10.1038/ngeo1765

Mulholland, M. R., Bronk, D. A., & Capone, D. G. (2004). Dinitrogen fixation and release of ammonium and dissolved organic nitrogen by *Trichodesmium* IMS101. *Aquatic Microbial Ecology*, *37*, 85–94. https://doi.org/10.3354/ame037085

Nan, F., Xue, H., & Yu, F. (2015). Kuroshio intrusion into the South China Sea: A review. *Progress in Oceanography*, *137*(2015), 314–333. https://doi.org/10.1016/j.pocean.2014.05.012

Patey, M. D., Rijkenberg, M. J., Statham, P. J., Stinchcombe, M. C., Achterberg, E. P., & Mowlem, M. (2008). Determination of nitrate and phosphate in seawater at nanomolar concentrations. *TrAC, Trends in Analytical Chemistry*, *27*(2), 169–182. https://doi.org/10.1016/j.trac.2007.12.006

Peltzer, E. T., & Hayward, N. A. (1996). Spatial and temporal variability of total organic carbon along 140°W in the equatorial Pacific Ocean in 1992. *Deep Sea Research Part II: Topical Studies in Oceanography*, *43*(4–6), 1155–1180. https://doi.org/10.1016/0967-0645(95)00014-3

Shaw, P. T., & Chao, S. Y. (1994). Surface circulation in the South China Sea. *Deep Sea Research Part I*, *41*(11–12), 1663–1683. https://doi.org/10.1016/0967-0637(94)90067-1

Shiah, F. K., Kao, S. J., & Liu, K. K. (1998). Bacterial production in the Western Equatorial Pacific: Implications of inorganic nutrient effects on dissolved organic carbon accumulation and consumption. *Bulletin of Marine Science -Miami*, *62*(3), 795–808. URl: http://ntour.ntou.edu.tw:8080/ir/handle/987654321/40989

Shiozaki, T., Kodama, T., & Furuya, K. (2014). Large-scale impact of the island mass effect through nitrogen fixation in the western South Pacific Ocean. *Geophysical Research Letters*, *41*, 2907–2913. https://doi.org/10.1002/2014GL059835

Siegel, D. A., Michaels, A. F., Sorensen, J. C., O'Brien, M. C., & Hammer, M. A. (1995). Seasonal variability of light availability and utilization in the Sargasso Sea. *Journal of Geophysical Research*, *100*(C5), 8695–8713. https://doi.org/10.1029/95JC00447

Smith, J. M., Chavez, F. P., & Francis, C. A. (2014). Ammonium uptake by phytoplankton regulates nitrification in the sunlit ocean. *PLoS One*, *9*(9), e108173. https://doi.org/10.1371/journal.pone.0108173

Tian, J. W., Yang, Q. X., Liang, X. F., Xie, L. L., Hu, D. X., Wang, F., & Qu, T. D. (2006). Observation of Luzon Strait transport. *Geophysical Research Letters*, *33*, L19607. https://doi.org/10.1029/2006GL026272

Tseng, C., Wong, G. T. F., Lin, I.-I., Wu, C.-R., & Liu, K.-K. (2005). A unique seasonal pattern in phytoplankton biomass in low-latitude waters in the South China Sea. *Geophysical Research Letters*, *32*, L08608. https://doi.org/10.1029/2004GL022111

Tyrrell, T. (1999). The relative influences of nitrogen and phosphorus on oceanic primary production. *Nature*, *400*(6744), 525–531. https://doi.org/10.1038/22941

Van Wambeke, F., Pfreundt, U., Barani, A., Berthelot, H., Moutin, T., Rodier, M., et al. (2016). Heterotrophic bacterial production and metabolic balance during the VAHINE mesocosm experiment in the New Caledonia lagoon. *Biogeosciences*, *13*(11), 3187–3202. https://doi.org/10.5194/bg-13-3187-2016

Wan, X. S., Sheng, H. X., Dai, M., Zhang, Y., Shi, D., Trull, T. W., et al. (2018). Ambient nitrate switches the ammonium consumption pathway in the euphotic ocean. *Nature Communications*, *9*(1), 915. https://doi.org/10.1038/s41467-018-03363-0

Ward, B. B. (2005). Temporal variability in nitrification rates and related biogeochemical factors in Monterey Bay, California, USA. *Marine Ecology Progress Series*, *292*, 97–109. https://doi.org/10.3354/meps292097

Ward, B. B. (2008). Nitrification in marine systems. In D. A. Capone, D. A. Bronk, M. R. Mulholland, & E. J. Carpenter (Eds.), *Nitrogen in the marine environment* (Vol. 5, pp. 199–261). London, UK: Academic Press. https://doi.org/10.1016/B978-0-12-372522-6.00005-0

Ward, B. B. (2011). Measurement and distribution of nitrification rates in the oceans. In J. N. Abelson & M. I. Simon (Eds.), *Methods in enzymology* (Vol. 486, pp. 307–323). London, UK: Academic Press. https://doi.org/10.1016/B978-0-12-381294-0.00013-4

Ward, B. B., Kilpatrick, K. A., Renger, E. H., & Eppley, R. W. (1989). Biological nitrogen cycling in the nitracline. *Limnology and Oceanography*, *34*(3), 493–513. https://doi.org/10.4319/lo.1989.34.3.0493

Wong, G. T., Ku, T. L., Mulholland, M., Tseng, C. M., & Wang, D. P. (2007). The South East Asian time-series study (SEATS) and the biogeochemistry of the South China Sea—An overview. *Deep Sea Research Part II: Topical Studies in Oceanography*, *54*(14-15), 1434–1447. https://doi.org/10.1016/j.dsr2.2007.05.012

Wu, K., Dai, M., Chen, J., Meng, F., Li, X., Liu, Z., et al. (2015). Dissolved organic carbon in the South China Sea and its exchange with the western Pacific Ocean. *Deep Sea Research Part II: Topical Studies in Oceanography*, *122*, 41–51. https://doi.org/10.1016/j.dsr2.2015.06.013

Yool, A., Martin, A. P., Fernández, C., & Clark, D. R. (2007). The significance of nitrification for oceanic new production. *Nature*, *447*(7147), 999–1002. https://doi.org/10.1038/nature05885

Zhang, Y., Zhao, Z., Dai, M., Jiao, N., & Herndl, G. J. (2014). Drivers shaping the diversity and biogeography of total and active bacterial communities in the South China Sea. *Molecular Ecology*, *23*(9), 2260–2274. https://doi.org/10.1111/mec.12739

Zhu, Y., Yuan, D., Huang, Y., Ma, J., & Feng, S. (2013). A sensitive flow-batch system for on board determination of ultra-trace ammonium in seawater: Method development and shipboard application. *Analytica Chimica Acta*, *794*, 47–54. https://doi.org/10.1016/j.aca.2013.08.009